AMORPHOUS PHASE CHARACTERIZATION THROUGH X-RAY DIFFRACTION PROFILE MODELING: IMPLICATIONS FOR AMORPHOUS PHASES IN GALE CRATER ROCKS AND SOILS.

C. N. Achilles[1], G. W. Downs[1], R. T. Downs[1], R. V. Morris[2], E. B. Rampe[2], D. W. Ming[2], S. J. Chipera[3], D. F. Blake[4], D. T. Vaniman[5], T. F. Bristow[4], A. S. Yen[8], S. M. Morrison[9], A. H. Treiman[10], P. I. Craig[5], R. M. Hazen[11], V. M. Tu[12], and N. Castle[10], [1]University of Arizona (cheriea@email.arizona.edu), [2]NASA JSC, [3]Chesapeake Energy, [4]NASA Ames, [5]Planetary Science Institute, [8]JPL/Caltech, [9]Carnegie Institution, [10]LPI, USRA, [12]Jacobs Technology.

Introduction: The CheMin X-ray diffraction instrument on the Mars Science Laboratory rover has analyzed 18 rock and soil samples in Gale crater. Diffraction data allow for the identification of major crystalline phases based on the positions and intensities of well-defined peaks and also provides information regarding amorphous and poorly-ordered materials based on the shape and positions of broad scattering humps [1]. The combination of diffraction data, elemental chemistry from APXS (Alpha Particle X-ray Spectrometer) and evolved gas analyses (EGA) from SAM (Sample Analysis at Mars) help constrain possible amorphous materials present in each sample (e.g., glass, opal, iron oxides, sulfates) [2-4] but are model dependent. We present a novel method to characterize amorphous material in diffraction data and, through this approach, aim to characterize the phases collectively producing the amorphous profiles in CheMin diffraction data. This method may be applied to any diffraction data from samples containing X-ray amorphous materials, not just CheMin datasets, but we restrict our discussion to martian-relevant amorphous phases and diffraction data measured by CheMin or CheMin-like instruments.

Amorphous Profile Modeling: Diffraction patterns result from the interaction of X-rays with materials in the path of the beam, including mineral phases and poorly- or non-crystalline materials (e.g., smectites, amorphous phases, sample holder materials). The structural periodicity of crystalline phases introduces sharp diffraction peaks whereas amorphous and poorly-ordered phases, lacking this periodicity, generate broad X-ray scattering profiles. Even though amorphous phase profiles do not exhibit sharp peaks, many amorphous materials exhibit unique scattering patterns as a consequence of variations in short-range structural order and chemistry. Diffraction patterns consisting of multiple amorphous phases are challenging to analyze, and identifying single phases within the mixture can be difficult to achieve with diffraction data alone.

Elemental chemistry provides important constraints on the abundance and composition of possible phases in amorphous mixtures. Additionally, EGA data may provide insight into phases that evolve H_2O, SO_2, and CO_2 upon heating. Consequently, identifying individual amorphous phases in the CheMin diffraction patterns that may be mixtures of several phases, benefits from constraints provided by APXS and SAM, measurements nominally acquired from the same sample. Our goal is to evaluate the identity and abundance of potential amorphous materials contributing to the broad scattering profiles in CheMin diffraction patterns.

Modeling analog amorphous phases. An atomic-level understanding of how short-range order affects the shape of amorphous profiles must first be investigated. We demonstrate that the diffraction profiles of amorphous phases with simple chemical compositions can be modeled by broadening the calculated diffraction peaks of selected minerals that have chemical compositions consistent with the amorphous material. The method thus directly associates chemical compositions with individual amorphous profiles. A library of ~35 analog amorphous materials of known composition, including glasses, sulfates, iron oxides, opal, and aluminosilicates, has been compiled. Diffraction data for each analog material was acquired on a CheMin-like laboratory diffractometer to best reproduce scattering profiles observed by the martian instrument. Crystalline diffraction patterns with Gaussian profiles are computed for each of the selected minerals in the model. A least squares optimization routine is used to vary the peak widths, scale factors, and background parameters for each computed crystalline pattern to best match the observed analog amorphous pattern. The analog data often include artifacts from Kapton or Mylar polymer windows used to hold the material during analysis. To account for the Kapton and/or Mylar scattering contribution, standard patterns of these polymers are included in the model and a scale factor is refined with the crystalline structure parameters. The optimized profile represents the sum of Gaussians for one or more crystalline phases that best simulate the analog amorphous scattering pattern.

Modeling results for two analog amorphous phases are displayed in Figures 1 and 2. A natural opal-A was modeled with broadened cristobalite and quartz peaks (Fig. 1). Figure 2 shows results for an amorphous Mg-sulfate that is modeled with broadened peaks from kieserite, sanderite, and Mg-oxysulfate data. Both optimized profiles show that the primary amorphous humps are well characterized by linear combinations of broadened crystalline phases. We propose that for these two chemically-simple samples, the short-range

order of the amorphous phase resembles the bonding environment of the minerals in each model. For example, cristobalite as the dominant phase in the opal-A model is consistent with cristobalite stacking disorder documented in natural opal-A samples [5]. A current concern is the poor fit at low 2θ. Figures 1 and 2 show Mylar (main peak ~18° 2θ) overcontributing to the model profile in order to best optimize the low angle intensity. Crystalline structures most relevant to the characterization of analog amorphous patterns lack peaks below 5° 2θ, making this region difficult to model with broadened peaks alone.

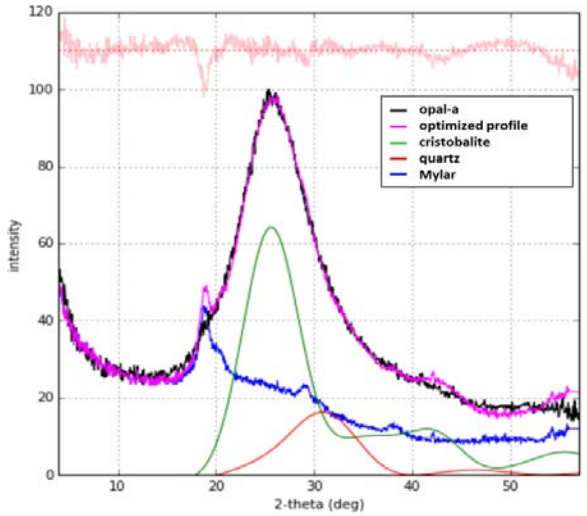

Figure 1. Opal-A (Australia) modeled with broadened cristobalite and quartz structure files.

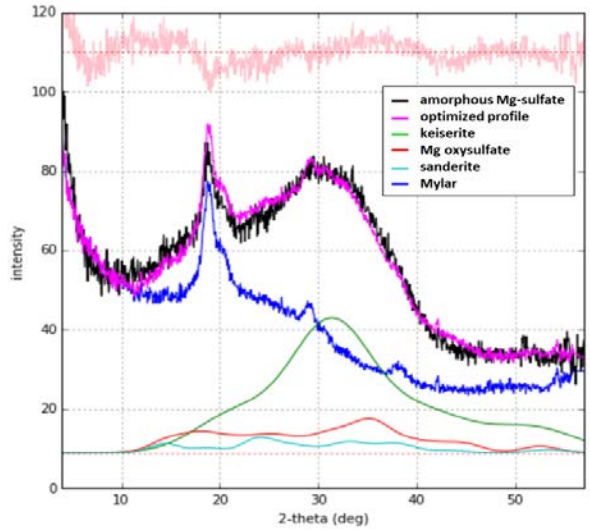

Figure 2. Amorphous Mg-sulfate modeled with three broadened Mg-sulfate structure files.

Modeling amorphous profiles – combining analog patterns and broadened crystalline phases. An alternate characterization of amorphous profiles involves combining analog amorphous patterns and broadened crystalline patterns. Analog patterns can be included in models where the amorphous profile has significant low-angle intensities, rather than relying on the broadened profiles of crystalline phases. Described previously, low-angle intensities are difficult to model with relevant, broadened crystalline structures. Thus, analog patterns are required to adequately represent the low-angle intensities present in amorphous profiles. An example of this approach is shown in Figure 3 where a natural opal pattern is modeled by a library analog opal (Australia, Fig. 1), broadened quartz, and non-broadened mineral data (to account for minor minerals present between 30° and 35° 2θ). The Kapton polymer peak (~6° 2θ) is not over scaled and most of the low-angle intensity is attributed to the analog opal-A pattern. The results shown in Figure 3 are a preliminary example of how CheMin diffraction data will be characterized in future models.

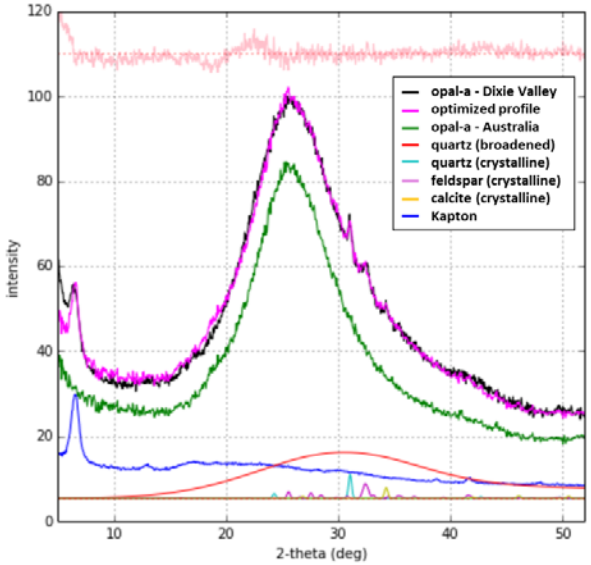

Figure 3. Natural, opal-A (Dixie Valley) pattern modeled with an opal-A amorphous pattern (Australia), broadened quartz, and crystalline phases.

The results presented in this abstract are the first steps in a new approach to modeling amorphous profiles observed in CheMin diffraction data. The addition of quantitative features, such as chemical constraints from APXS and phase predictions from SAM, are essential parameters for applications to CheMin data and is part of the ongoing work aimed at applying these results to CheMin amorphous profiles.

References: [1] Blake, D. F. et al. (2012) *Space Sci. Rev. 170*, 401-478. [2] Campbell, J. L. et al. (2012) *Space Sci. Rev. 170*, 319-340. [3] Mahaffy, P. R. et al. (2012) *Space Sci. Rev. 170*, 401-478. [4] Sutter, B. et al. (2017) *JGR 122*. [5] Elzea, J. M. and Rice, S. B. (1996) *Clay and Clay Min. 44*, 492-500.